Global Journal of Science Frontier Research: F
Mathematics and Decision Sciences
Volume 14 Issue 3 Version 1.0 Year 2014
Type : Double Blind Peer Reviewed International Research Journal
Publisher: Global Journals Inc. (USA)
Online ISSN: 2249-4626 & Print ISSN: 0975-5896

Effect of Buoyancy Force on the flow field in a Triangular Cavity

By Abdul Halim Bhuiyan, Sayeda Fahmida Ferdousi & M.A. Alim
Bangladesh University of Engineering and Technology, Bangladesh

Abstract- In this paper, the effect of buoyancy force in a triangular enclosure are studied numerically. The governing differential equations are solved by using finite element method (weighted-residual method). Here the left wall of the triangle is assumed to be adiabatic, the right and horizontal wall are kept at cold and heated respectively. Also all the wall are assumed to be no-slip condition. The effective governing dimensionless parameters for this problem are Rayleigh number, Prandtl number and Hartmann number.

Keywords: *buoyancy force; finite element method; hartmann number; triangular cavity.*

GJSFR-F Classification : *MSC 2010: 57Q15*

EFFECTOFBUOYANCYFORCEONTHEFLOWFIELDINATRIANGULARCAVITY

Notes

Effect of Buoyancy Force on the Flow Field in a Triangular Cavity

Abdul Halim Bhuiyan [α], Sayeda Fahmida Ferdousi [σ] & M.A. Alim [ρ]

Abstract- In this paper, the effect of buoyancy force in a triangular enclosure are studied numerically. The governing differential equations are solved by using finite element method (weighted-residual method). Here the left wall of the triangle is assumed to be adiabatic, the right and horizontal wall are kept at cold and heated respectively. Also all the wall are assumed to be no-slip condition. The effective governing dimensionless parameters for this problem are Rayleigh number, Prandtl number and Hartmann number.

Keywords: buoyancy force; finite element method; hartmann number; triangular cavity.

I. Introduction

Natural convection heat transfer and fluid flow are widely studied topics in engineering due to their practical importance as reviewed by [1] and [2]. Nearly forty years ago as in [3] and [4] studied the natural convection in enclosures with internal heat generation occurs in nuclear reactors and geothermal heat extraction processes. Based on technological applications of internal heat generation problems in nuclear reactors and geometrical applications, as in [5] and [6] obtained several solutions. Besides regular geometries such as square or rectangle, many studies wavy-walled enclosures with or without internal heat generation. Natural convection in wavy enclosures with volumetric heat sources was investigated by [7]. They found that, both the function of wavy wall and the ratio of internal Rayleigh number Ra_I to external Rayleigh number Ra_E affect the heat transfer and fluid flow significantly. The heat transfer is predicted to be a decreasing function of waviness of the top and bottom walls in case of

$$\frac{Ra_I}{Ra_E} > 1 \text{ and } \frac{Ra_I}{Ra_E} < 1$$

Most of the enclosures commonly used in industries are cylindrical, rectangular, trapezoidal and triangular etc. In recent years, triangular enclosures have received a considerable attention because of its applicability in various fields. Finite element analysis of natural convection in triangular enclosure was studied by [8]. They found that at low Rayleigh numbers $(Ra \leq 10^4)$, the isotherms are almost parallel near the bottom portion of the triangular enclosure while at $Ra = 10^5$, the isotherms are more distorted. This is because the heat transfer is primarily

Author α: Department of Mathematics Bangladesh University of Engineering and Technology, Bangladesh.
e-mail: ahalim@math.buet.ac.bd
Author σ: Department of Natural Sciences Stamford University Bangladesh, Bangladesh. e-mail: fahmida_ferdousi@yahoo.com
Author ρ: Department of Mathematics Bangladesh University of Engineering and Technology, Bangladesh.
e-mail: maalim@math.buet.ac.bd

due to conduction for lower values of Rayleigh number. As Rayleigh number increases, there is a change from conduction dominant region to convection dominant region, and the critical Rayleigh number corresponding to on-set of convection is obtained. The main objective of this paper is to study natural convection heat transfer in a triangular shape enclosure. From the above literatures, the aim of present investigation is to investigate the effect of buoyancy force in triangular shape enclosure. The results are presented in terms of streamlines, isotherms, velocity profiles, temperature profiles and local Nusselt number.

Notes

II. Model and Mathematical Formulation

The Figure 1 shows a schematic diagram and the coordinates of a two-dimensional triangular cavity, where the bottom wall is maintained at a uniform temperature T_h and the left wall maintained adiabatic whereas right wall T_c colder. The fluid is permeated by a uniform magnetic field B_0 which is applied normal to the direction of the flow and the gravitational force (g) acts in the vertically downward direction.

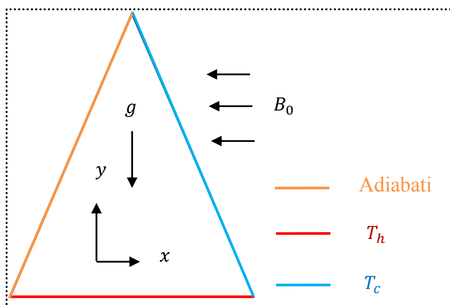

Figure 1 : The flow configuration and coordinate system

The fluid properties, including the electrical conductivity, are considered to be constant, except for the density, so that the Boussinesq approximation is used. Neglecting the radiation mode of the heat transfer and Joule heating, the governing equations for mass, momentum and energy of a steady two-dimensional natural convection flow in a triangular cavity are as follows:

$$\frac{\partial u}{\partial x}+\frac{\partial v}{\partial y}=0 \tag{1}$$

$$\rho\left(u\frac{\partial u}{\partial x}+v\frac{\partial u}{\partial y}\right)=-\frac{\partial p}{\partial x}+\mu\left(\frac{\partial^2 u}{\partial x^2}+\frac{\partial^2 u}{\partial y^2}\right) \tag{2}$$

$$\rho\left(u\frac{\partial v}{\partial x}+v\frac{\partial v}{\partial y}\right)=-\frac{\partial p}{\partial y}+\mu\left(\frac{\partial^2 v}{\partial x^2}+\frac{\partial^2 v}{\partial y^2}\right)+\rho g\beta\left(T-T_c\right)-\sigma B_0{}^2 v \tag{3}$$

$$u\frac{\partial T}{\partial x}+v\frac{\partial T}{\partial y}=\alpha\left(\frac{\partial^2 T}{\partial x^2}+\frac{\partial^2 T}{\partial y^2}\right) \tag{4}$$

The governing equations are nondimensionalized using the following dimensionless variables:

$$X=\frac{x}{L},\quad Y=\frac{y}{L},\quad U=\frac{uL}{\alpha},\quad V=\frac{vL}{\alpha},$$
$$P=\frac{pL^2}{\rho\alpha^2},\theta=\frac{T-T_c}{T_h-T_c}\ ,\quad \sigma=\frac{\rho^2\alpha}{L^2},\quad \alpha=\frac{k}{\rho C_p}$$

Notes

Introducing the above dimensionless variables, the following dimensionless forms of the governing equations are obtained as follows:

$$\frac{\partial U}{\partial X}+\frac{\partial V}{\partial Y}=0 \tag{5}$$

$$U\frac{\partial U}{\partial X}+V\frac{\partial U}{\partial Y}=-\frac{\partial P}{\partial X}+\Pr\left(\frac{\partial^2 U}{\partial X^2}+\frac{\partial^2 U}{\partial Y^2}\right) \tag{6}$$

$$U\frac{\partial V}{\partial X}+V\frac{\partial V}{\partial Y}=-\frac{\partial P}{\partial Y}+\Pr\left(\frac{\partial^2 V}{\partial X^2}+\frac{\partial^2 V}{\partial Y^2}\right)+\frac{Ra}{\Pr}\theta\ -\ Ha^2\Pr V \tag{7}$$

$$U\frac{\partial \theta}{\partial X}+V\frac{\partial \theta}{\partial Y}=\frac{\partial^2 \theta}{\partial X^2}+\frac{\partial^2 \theta}{\partial Y^2} \tag{8}$$

Here Pr is the Prandtl number, *Ra* is the Rayleigh number and *Ha* is the Hartmann number, which are defined as:

$$\Pr=\frac{\nu}{\alpha},\ Ha^2=\frac{\sigma B_0{}^2L^2}{\mu}\ ,Ra=\frac{g\beta L^3\left(T_h-T_c\right)\Pr}{\nu^2}$$

The corresponding boundary conditions then take the following form:

$$U=V=0,\ \theta=1\left(\text{on the bottom wall}\right)$$
$$U=V=0,\ \theta=0\ (\text{on the right wall})$$
$$U=V=0,\ \frac{\partial\theta}{\partial N}=0\ (\text{at left wall})$$
$$P=0\left(\begin{array}{c}\text{fluid pressure, at the inside and on the}\\ \text{wall of the enclosure}\end{array}\right)$$

III. Numerical Procedure

The Galerkin weighted residual method of finite element formulation is used to solve the dimensionless governing equations with the boundary conditions. This technique is well described by [9] and [10]. In this method, the solution domain is discretized into finite element meshes and then the nonlinear governing equations are transferred into a system of integral equations by applying the Galerkin weighted residual method. Gauss quadrature method is used to perform the integration involved in each term of these equations. The nonlinear algebraic equations which are obtained are modified by imposition of boundary conditions and Newton's method is used to transform these modified equations into linear algebraic equations, and then these linear equations are solved by applying the triangular factorization method.

Global Journal of Science Frontier Research (F) Volume XIV Issue III Version I Year 2014

Notes

IV. Code Validation

In order to verify the accuracy of the numerical results which are obtained throughout the present study are compared with the previously published results. The present results of streamlines and isotherms are compared with that of [11] while uniformly heated left wall $\theta(0,Y)=1$ and cooled right inclined wall $\theta(X,Y)=0, \forall X+Y=1$ with Pr = 1000 and Ra=10^5 and obtained good agreement which is shown in Fig. 2.

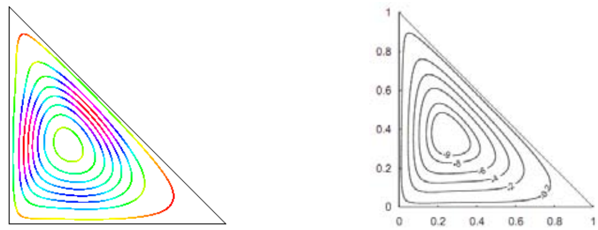

Present work Reference [11]

Figure 2 (a) : Obtained results for Streamlines

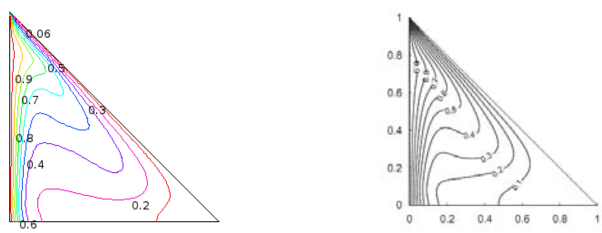

Present work Reference [11]

Figure 2 (b) : Obtained results Isotherms

V. Results and Discussion

In this section, results of the numerical study on magneto hydrodynamic buoyancy force in a triangular cavity filled with an electric conductive fluid with Pr = 0.71 are presented. The results have been obtained for the Rayleigh number ranging from 10^4 to 10^6 and the three Hartman numbers 0, 50 and 100. The results are presented in terms of streamlines and isotherms inside the cavity, the horizontal velocity component, temperature and the local Nusselt number along the vertical centerline X=0.5 of the cavity. Figures 3 and 4 presents the effects of the Rayleigh number Ra=10^4 on the flow field for different Hartmann number (a) Ha=0; (b) Ha=50; (c) Ha=100. They are illustrated by streamlines (Fig. 3) and isotherms (Fig. 4) respectively. The results for Ra=10^4 and different Hartmann number given in Fig. 3 and it is found that a triangle shape flow distribution is formed. The main flow moves in clockwise direction and for Ha=0 it is not broken anywhere in the triangle. Also a small cell is formed at the centre of the triangle and in this case flow becomes uniform within the whole enclosure. The flow streamlines fill the whole enclosure geometry except at the corners. Also a large velocity is distributed uniformly within the whole enclosure for Ha=0. As the value of the Hartmann number increases to 0 to 100, the flow velocity decreases due to the insulated edge and the flow started too broken due to the cold edge. Finally for Ha=100 the flow velocity become very weak due to the insulated edge and the last cell of the flow is broken and twisted backward to the adiabatic edge. The flow becomes motionless at these parts due to the insulated edge. The isotherm lines showed in Fig. 4 indicates similar distribution with a benchmark problem of differentially heated cavity except at the insulated edge. Figure 4(a) shows that, the boundary layer decreases from heated edge to cold edge and isotherms lines are started bending due to insulated edge and become smother near the cold edge for *Ha*=0. As we increase the Hartmann number in this case the lines become smothering but the boundary layer increases. Figures 5 and 6 shows the streamlines and isotherm lines for (a) *Ha*=0, (b) *Ha*=50 and (c) *Ha*=100 while Pr=0.71 and $Ra=10^5$. As we increase Rayleigh number $Ra=10^5$, the changes in streamlines within the triangular enclosure are negligible (same as above) but the isotherm lines are highly bending at the middle of the triangular enclosure and become smother due to the cold edge for *Ha*=0. Also the boundary layer become decreases due to the cold edge for *Ha* =0. But as we increase Hartmann number the bending lines become smother and the boundary layer increases. Finally Fig. 7 and Fig. 8 shows the streamlines and isotherms for (a) *Ha*=0, (b) *Ha*=50 and (c) *Ha*=100 while Pr=0.71 and $Ra=10^6$. For $Ra=10^6$, the flow velocity become weak and streamlines are bended due to the insulated edge, isotherms lines are highly bended at the middle of the triangular enclosure and become more smother near the cold edge for *Ha*=0. As we increase Hartmann number the isotherm lines becomes smother and the boundary layer increases. Thus, if we increase both Hartmann number and Rayleigh number the flow become weak and boundary layer increases. The local Nusselt number along the vertical centerline X=0.5 of the enclosure is plotted in Figs. 9(a) - 9(c) for different values of Rayleigh number 10^4,10^5 and 10^6. It is also plotted for different values of Hartmann number. The maximum value of the local Nusselt number occur around Y= 0.7 for $Ra=10^6$ and *Ha*=0. Comparison of Fig. 9(b) and 9(c) indicates that the maximum value of local Nusselt number decreases for *Ha*=0 and *Ha*=100 respectively while $Ra=10^6$.

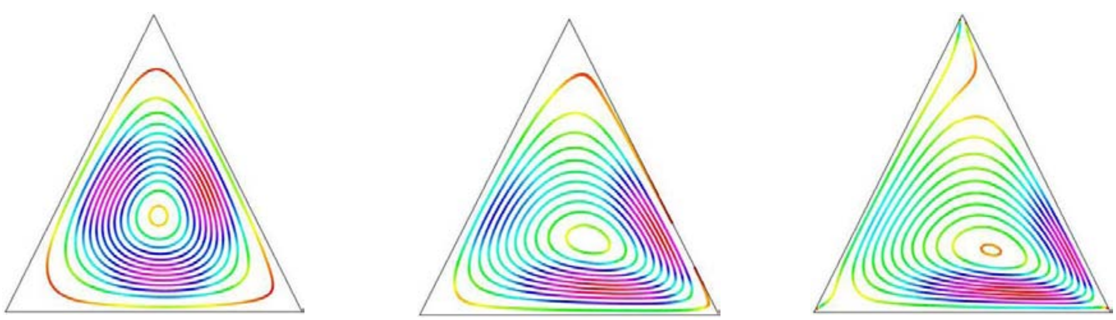

(a) (b) (c)

Figure 3 : Streamlines for (a) *Ha*=0; (b) *Ha*=50; (c) *Ha*=100 while Pr=0.71 and $Ra=10^4$

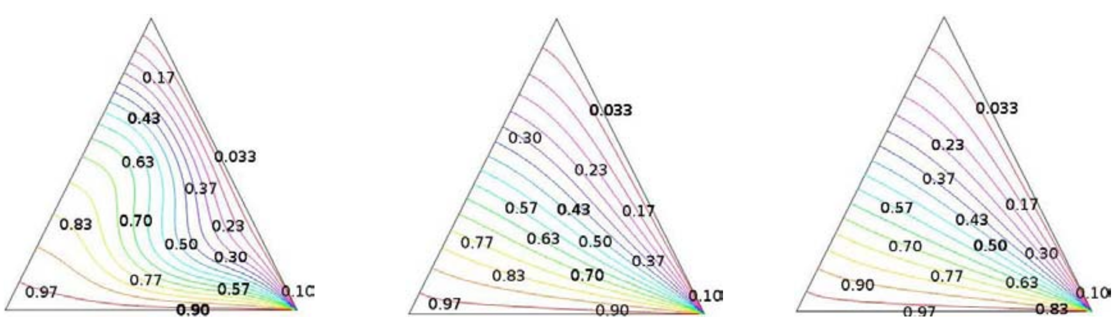

(a) (b) (c)

Figure 4 : Isotherms for (a) *Ha*=0; (b) *Ha*=50; (c) *Ha*=100 while Pr=0.71 and $Ra=10^4$

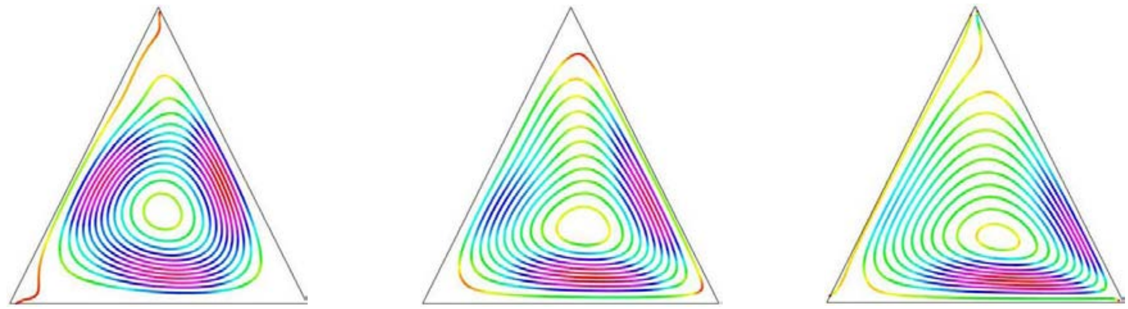

(a) (b) (c)

Figure 5 : Streamlines for (a) *Ha*=0; (b) *Ha*=50; (c) *Ha*=100 while Pr=0.71 and $Ra=10^4$

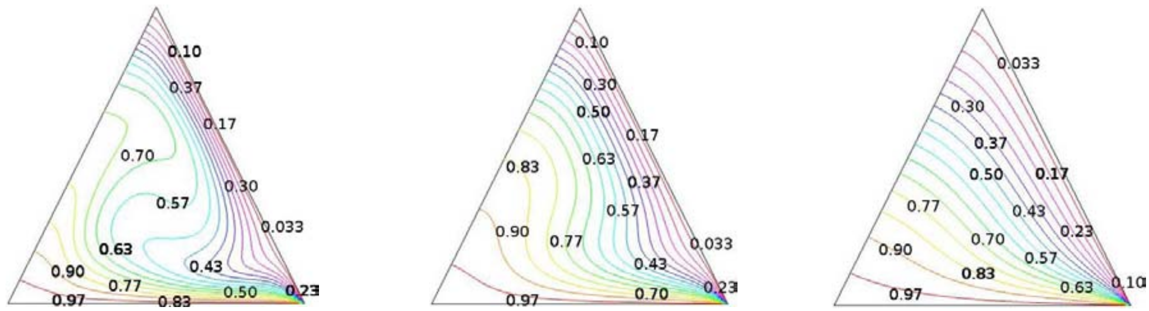

(a) (b) (c)

Figure 6 : Isotherms for (a) *Ha*=0; (b) *Ha*=50; (c) *Ha*=100 while Pr=0.71 and $Ra=10^5$

The profiles of the dimensionless X-component of velocity *U* versus the vertical co-ordinate are plotted at the middle of the enclosure based on the X-axis in Fig. 10(a) to (c). They are plotted for different curved length of the enclosure. It is clearly seen in Fig 10(a), for *Ha*=0 the highest velocity is obtained for $Ra=10^6$. The velocity profiles indicate the most important parameter on the flow field is the shape of the enclosure. Figures 11(a) -11 (c) indicate the temperature profile versus the vertical co-ordinate. It is clear from the above figure that, for $Ra=10^4$ we get the smoothed temperature profile. As we increase Hartmann number the profile become more smother.

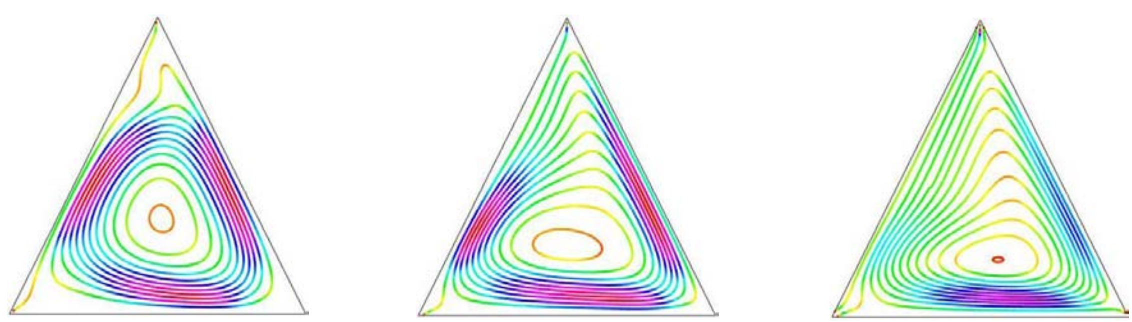

(a) (b) (c)

Figure 7 : Streamlines for (a) *Ha*=0; (b) *Ha*=50; (c) *Ha*=100 while Pr=0.71 and $Ra=10^6$

Notes

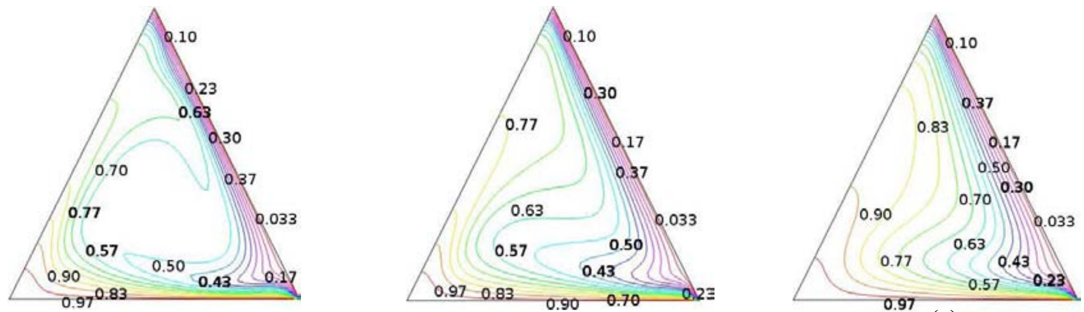

Figure 8 : Isotherms for (a) *Ha*=0; (b) *Ha*=50; (c) *Ha*=100 while Pr=0.71 and *Ra*=10^6

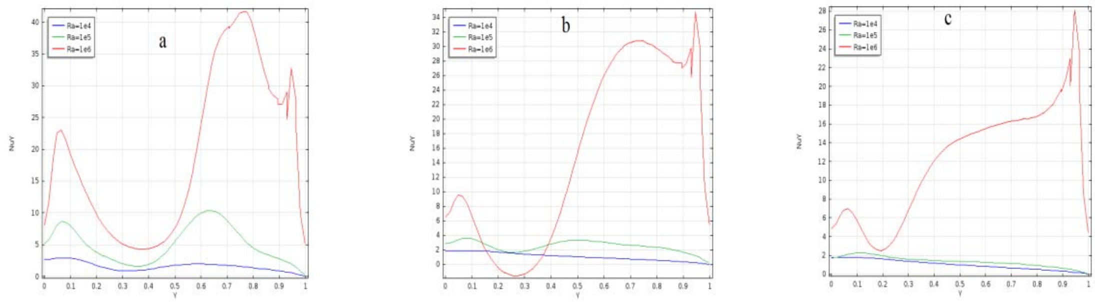

Figure 9 : Variation of local Nusselt number along the vertical centerline X=0.5 for different Rayleigh number with Pr=0.71 for (a) *Ha*=0, (b) *Ha* = 50 and (c) *Ha*=100.

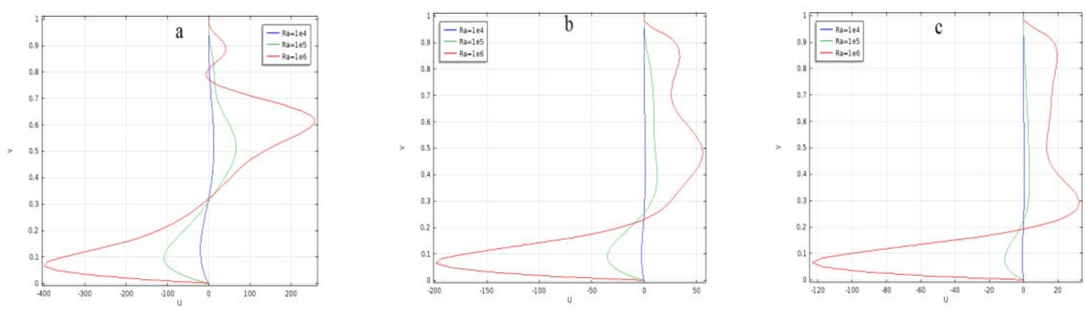

Figure 10 : Variation of velocity profiles along the vertical centerline X=0.5 at different Rayleigh number with Pr=0.71 for a) *Ha*=0, b) *Ha*=50 and c) *Ha*=100.

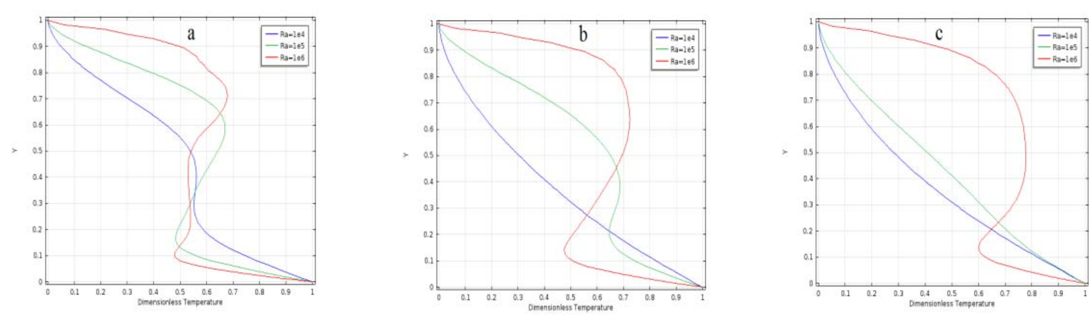

Figure 11 : Variation of temperature profiles along the vertical centerline X=0.5 at different Rayleigh number with Pr=0.71 for a) *Ha*=0, b) *Ha*=50 and c) *Ha*=100.

VI. Conclusion

Effect of buoyancy force on the flow field in a triangular cavity with uniform magnetic field B_0 which is applied normal to the direction of the flow was studied numerically. The governing equations of mass, momentum and energy were solved using the Galerkin weighted residual method of finite element formulation. As indicated above that the governing parameters were the Prandtl number Pr, the Rayleigh number *Ra* and the Hartmann number *Ha*. The effects of Rayleigh number *Ra* with the variations Hartmann number *Ha* on the flow field have been studied in detail while Prandtl number Pr=0.71. From the present investigation the following conclusions may be drawn as: if the Rayleigh number increases, the local Nusselt number increases without the effect of magnetic field whereas the local Nusselt number slowly increases with the increase of Rayleigh number with applying the effect of magnetic field.

Notes

References Références Referencias

1. G. de Vahl Davis and I.P. Jones, "Natural convection in a square cavity: a comparison exercise", Int. J. Num. Methods Fluid, vol. 3, pp. 227-249, 1983.
2. S. Ostrach, "Natural convection in enclosures", J. Heat Transfer, vol. 110, pp. 1175-1190, 1988.
3. F.A. Kulacki and R.J. Goldstein, "Thermal convection in a horizontal fluid layer with uniform volumetric energy sources", J. Fluid Mech., vol. 55, pp. 271-287, 1972.
4. F.A. Kulacki and M.E. Nagle, "Natural convection in a horizontal fluid layer with volumetric energy sources", J. Heat Transfer, vol. 97, pp. 204-211, 1975.
5. S. Acharya and R.J. Goldstein, "Natural convection in an externally heated vertical or inclined square box containing internal energy sources", J. Heat Transfer, vol. 107, pp. 855-866, 1985.
6. J.H. Lee and R.J. Goldstein, "An experimental study on natural convection heat transfer in an inclined square enclosure containing internal energy sources", J. Heat Transfer, vol. 110, pp. 345-349, 1988.
7. Hakan F. Oztop, Eiyad Abu-Nada, Yasin Varol and Ali Chakma, "Natural convection in wavy enclosures with volumetric heat sources", Int. J. Thermal sciences, vol. 50, pp. 502-514, 2011.
8. Tanmay Basak, S. Roy and Ch. Thirumalesha," Finite element analysis of natural convection in a triangular enclosure: Effects of various thermal boundary conditions", J. Chemical Engineering Science, vol. 62, pp. 2623-2640, 2007.
9. C. Taylor and P. Hood, "A numerical solution of the Navier-Stokes Equations using finite element technique, Computer and Fluids", vol. 1, No. 1, pp. 73-89, 1973.
10. P. Dechaumphai, "Finite Element Method in Engineering, Second edition, Chulalongkorn University Press", Bangkok, 1999.
11. Tanmay Basak, S. Roy and Ch. Thirumalesha, "Finite element analysis of natural convection in a triangular enclosure: Effects of various thermal boundary conditions", Chemical Engineering Science, vol. 62, pp. 2623–2640, 2007.